Progress In Electromagnetics Research, Vol. 145, 229–240, 2014

Setup for Simultaneous Microwave Heating and Real-Time Spectrofluorometric Measurements in Biological Systems

Sophie Kohler[1], Nicolas Ticaud[1], Maria-Minodora Iordache[2], Mihaela G. Moisescu[2], Tudor Savopol[2, *], Philippe Leveque[1], and Delia Arnaud-Cormos[1]

Abstract—In this paper, a delivery system allowing simultaneous microwave heating and real-time spectrofluorometric measurements in biological systems is proposed and characterized. This system is used to investigate the phase behavior of lipid bilayers from about 15°C to 45°C. The delivery system is based on an open transverse electromagnetic (TEM) cell combined with a spectrofluorometer via an optical cable system. A numerical and experimental dosimetry of the delivery system is conducted. The Specific Absorption Rate (SAR) efficiency of the system is 26.1 ± 2.1 W/kg/W. Spectrofluorometric measurements on Laurdan labeled small unilamellar vesicles (SUVs) are carried out. Generalized polarization (GP) of the SUV's membrane is obtained from the fluorescence intensities measured at two emission wavelengths.

1. INTRODUCTION

Heating is a well-known effect of the interaction between microwaves and dielectric materials. At 2.45 GHz, a standard frequency for industrial, medical and scientific purposes, heating is attributed to the inability of permanent electric dipoles (e.g., water molecules) to rotate fast enough to line up with the continuously reversing electric field (E-field). The loss mechanisms result in power dissipation. Advantages of microwave heating over conventional heating include faster heating, higher efficiency, possibility of better temperature control and better volumetric temperature homogeneity [1–3].

Some properties of the plasma membrane of biological cells vary as a function of temperature. In particular, the transition from solid or gel phase (ordered phase) to liquid-crystalline phase (unordered phase) can be characterized under microwave heating [4, 5]. One specific parameter accounting for the thermal behavior of membranes is the so-called generalized polarization (GP). The measurement of this parameter is usually conducted by processing the emission spectra of the lipophilic fluorescent probe Laurdan at different temperatures [6, 7]. Laurdan inserts in the hydrophobic core of the membrane. The shape of its emission spectrum depends on the polarity of the environment; as the membrane is heated, when it reaches the critical phase transition temperature, there is an important water influx in the membrane leading to significant modifications of the fluorescence spectrum of Laurdan.

In classical fluorometers, a rectangular plastic cuvette contains the samples (e.g., cellular or artificial vesicles suspensions). The cuvette is placed in a thermostated holder associated with Peltier elements for temperature control, in the optical path of the fluorometer. In microwave experiments, biological samples are typically exposed to electromagnetic fields (EMF) via radiating, propagating or resonant systems [8].

Several types of systems have been developed that allow simultaneous microwave exposure and real-time measurement of samples. Exposure systems for electrophysiological recordings have been

Received 7 November 2013, Accepted 8 March 2014, Scheduled 28 March 2014

* Corresponding author: Tudor Savopol (tsavopol@umf.ro).

[1] Xlim Research Institute, University of Limoges and CNRS, 123 Avenue Albert Thomas, Limoges F-87060, France. [2] Department of Biophysics and Cellular Biotechnology, Carol Davila University of Medicine and Pharmacy, 8 Eroilor Sanitari Blv., P. O. Box 35-43, Bucharest, Romania.

designed using a coplanar waveguide, using either an inverted microscope or a metallic electrode tip for physiological recordings [9, 10]. These systems are well adapted for cells or tissues contained in a Petri dish. For studies of neural networks, an exposure system for micro-electrode arrays (MEA) was developed by positioning this device in a waveguide [11]. In this case, neurons were cultured on electrodes at the bottom of the MEA, which allowed the extracellular recording of neuronal activity.

Waveguide-based systems have also been used to study the nonthermal effects of microwaves on skeletal muscle [12]. This system included a vertical organ bath, which allowed the muscle sample to be kept under physiological conditions when placed inside the waveguide. The stimuli for muscle contractions were generated by two platinum electrodes and continuously measured before, during and after the microwave exposure.

An exposure system for the study of microwave field effects on liposomes was proposed in [13]. This system was inserted in a spectrophotometer and was based on a modified stripe line adjacent to the cuvette and thermoregulatory cell.

The exposure systems reviewed above were not developed and characterized for real-time spectrofluorimetric applications with simultaneous microwave exposure and sample measurement. Moreover, some of these highly localized systems are less adapted for exposing the volume in a cuvette for fluorescence measurements and with global increases in the temperature higher than 25°C.

To achieve simultaneous real-time fluorometric measurements and microwave exposure in a cuvette, a specific delivery system was developed [14]. In that configuration, the sample was exposed to EMF via an open coaxial cable, which was vertically inserted into the biological sample, in the center of the cuvette. This system had two main drawbacks: a) the existence of a hot spot occurring in the vicinity of the coaxial cable tip, and b) the presence of the coaxial cable in the biological sample. To avoid these disadvantages, a delivery system based on wave propagation can be used. A system based on a open transverse electromagnetic (TEM) cell was developed for imaging temperature by using a fluorescent molecular probe with thermosensitive properties [15]. This study focused on adherent cells cultured at the bottom layer of the Petri dish used as a biological holder. This system was adapted for measurements using a microscope. It was not designed and characterized for heating in a cuvette for fluorescence measurements. As developed, it was not readily portable for external measurements using an optical guiding system. The TEM cell was also used to demonstrate the ability of an electrooptic probe for simultaneous E-field and temperature measurements [16]. However, these previous works need to be reviewed and completed due to the requirement of new holder and frequency for this study.

In this paper, a delivery system allowing simultaneous 2.45 GHz microwave exposure and real-time spectrofluorometric measurements of samples is proposed. The thermal and electromagnetic properties of the sample are characterized through temperature and E-field measurements. In addition, spectrofluorometric measurements are shown to validate the setup.

The paper is organized as follows. In Section 2, the setup is described and the methods for the experimental and numerical dosimetry are presented in terms of SAR and the temperature distribution. The protocol for the fluorescence measurements is also described in Section 2. The experimental and numerical results are detailed in Section 3. A conclusion is given in Section 4.

2. MATERIAL AND METHODS

2.1. Exposure Setup

The experimental setup developed is in Fig. 1. The setup is composed of a 2.45 GHz microwave generator (MPG4, Opthos Instruments Inc., MD, USA) delivering 120 W of maximum power. A circulator (E3 2425 01, Sodhy, France) with a 50 Ω load (CA 50NM, Sodhy, France) on one port was used to isolate the generator from the potential reflected power. In order to measure the incident and reflected powers, a 30 dB bidirectional coupler (CD E 2425-2N, Sodhy, France) was inserted between the microwave generator and the delivery system. Power detectors (HP 8472A, Hewlett Packard, CA, USA) were connected to the bidirectional coupler and to a PC-based digital storage oscilloscope (PCS500, Velleman, Belgium) for the monitoring of the incident and reflected powers. To avoid saturation of the incident power detector, a 6 dB attenuator (PE7014-6, Pasternack, CA, USA) was added. The microwave power was adjusted by changing the generator power associated to a variable attenuator (0–20 dB, PE7065-3, Pasternack, CA, USA).

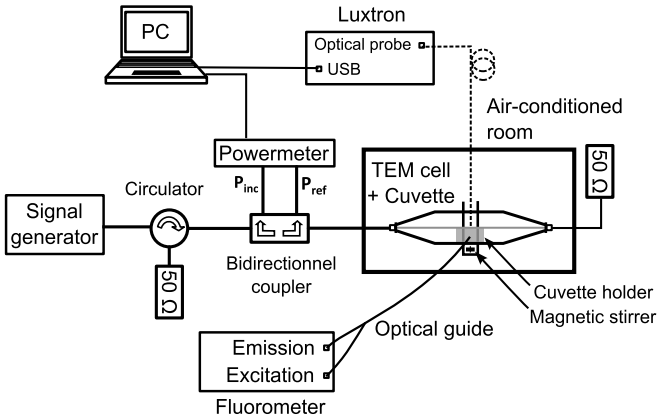

Figure 1. Schematic of the microwave exposure system containing: the power source, the delivery system and the monitoring assembly (powermeter, thermometer, oscilloscope, PC).

Figure 2 shows a photo and a schematic representation of the delivery system. It consists of an open TEM cell [17–19]. The TEM cell is a transmission line composed of a tapered flat inner conductor forming a septum, surrounded by two tapered and grounded metallic walls. A 12 mm × 12 mm × 40 mm plastic cuvette with optically clear walls was used as a container for the biological sample. The cuvette was filled with 2.8 ml of either double-distilled water or of a suspension of small unilamellar vesicles (SUVs). The cuvette was vertically placed through apertures in the TEM cell walls. For impedance matching, the output port of the TEM cell was connected to a 50 Ω load (CA 50NM, Sodhy, France).

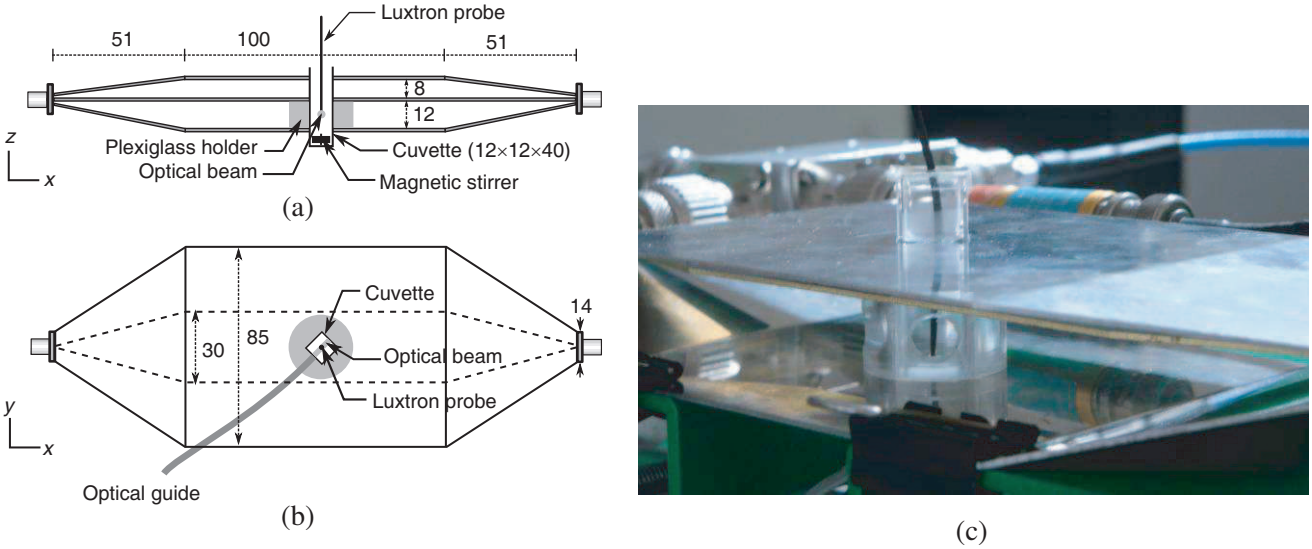

Figure 2. Photo and schematic of the cuvette within the TEM cell: (a) side view, (b) top view and (c) photo.

In order to homogenize the solution, a crosshead magnetic stirrer placed at the bottom of the cuvette was used for continuously stirring the solution. The stirrer velocity was 350 rotations per minute. As shown in Fig. 2, the cuvette was positioned 5 mm below the TEM cell with the stirrer being thus placed below the lower metallic wall of the TEM. This limited the disturbance of the stirrer on the *E*-field propagation inside the TEM cell.

To characterize the temperature in the solution, a fiber-optic probe (Luxtron One, Luxtron, CA, USA) was vertically inserted into the cuvette. The temperature was recorded at a sampling rate of 4 Hz and displayed in real-time on a PC.

The delivery system was placed in a 33 cm × 28 cm × 21 cm air-conditioned unit. Holes were drilled in the box for connecting the TEM cell via coaxial cables, inserting the temperature probe and the optical guiding system for fluorescence measurements. A Horiba Fluorolog 2 (Horiba Scientific, Edison, NJ, USA) spectrofluorometer was optically connected to the microwave delivery system via the optical guiding system (F-3000 Fiber Optic Mount, Horiba Scientific). One end of the optical guide was applied on the clear face of the cuvette using a plexiglass mount. The other end was split into two branches connected to the excitation output and emission input slits of the fluorometer monochromators, respectively.

2.2. Numerical Dosimetry

A numerical simulation based on a 3D finite-difference time-domain (FDTD) method was conducted to compute the electromagnetic fields in the exposure system [20, 21]. The algorithm was developed at XLIM Research Institute and has been validated by previous work [18, 22, 23]. The FDTD method was applied to solve the time-dependent Maxwell's equations in differential form, the latter governing the propagation of electromagnetic waves and their interaction with matter. The FDTD technique consists in discretizing the space and time derivatives using the central difference method. At each time step of the algorithm, both the electric and magnetic components of the electromagnetic fields are computed over the spatial grid of the simulated volume. The knowledge of the electromagnetic fields was required in the three spatial dimensions because of the complex geometry of the exposure system and the target.

The volume simulated with the FDTD solver was composed of the TEM cell and the cuvette filled with water. A 50 Ω localized electromagnetic generator, using the thin wire formalism, was connected at the input port of the TEM cell while the output port was terminated in a 50 Ω load. The metallic parts of the TEM cell were considered as perfect conductors. The relative dielectric permittivity of the solution was 75.6 and the electrical conductivity was 2.5 S/m at 2.45 GHz. To prevent wave's reflection at the boundaries of the computational domain, perfectly matched layers (PMLs) were added to the domain [24]. The number of PML layers was set to 13.

The FDTD requires a spatial resolution that is at least ten times smaller than the shortest wavelength in the simulation. At 2.45 GHz, the wavelength of the electromagnetic field is 12.2 cm in free space and about 1.5 cm in a dielectric material with a relative permittivity of 75. We chose to mesh the simulated volume with a uniform grid of 0.25 mm × 0.25 mm × 0.25 mm. Thus, the volume comprised 835 × 181 × 117 unit cells for a total computing memory size of 1.07 GB. A spatial symmetry along the y-axis was used to reduce the computational volume. The upper limit of the increment time step (Δt) is related to the size of the spatial mesh (Δx, Δy, Δz) as imposed by the Courant stability criterion:

$$\Delta t \leq \frac{1}{c\sqrt{\left(\frac{1}{\Delta x^2}+\frac{1}{\Delta y^2}+\frac{1}{\Delta z^2}\right)}} \tag{1}$$

where c is the celerity of electromagnetic waves in free space. The time-step was set to 0.36 ps and the total simulated time was 1.8 ns. A complete simulation required 660 s on a NEC-SX8 computer cluster.

From the discrete Fourier transform of the electric field components, SAR was calculated in each unit cell. The SAR (W/kg) is defined as the time derivative of the incremental energy ∂W absorbed by or dissipated in an incremental mass ∂m contained in a volume element ∂V of a given mass density ρ (kg/m^3) [25]:

$$SAR = \frac{\partial}{\partial t}\left(\frac{\partial W}{\rho \partial V}\right) \tag{2}$$

Since $\partial W/\partial t$ is equivalent to power (W), the SAR is related to the E-field amplitude, $|E|$:

$$SAR = \frac{\sigma |E|^2}{\rho} \tag{3}$$

where ρ is the mass density (kg/m^3) and σ the electrical conductivity (S/m) of the exposed sample. In each elementary cell, the E-field and the SAR were computed. The calorific dissipated power (σE^2 in W/m^3) is directly proportional to the SAR and induces temperature elevation.

In this work, the numerical simulation was limited to the electromagnetic fields computation. Thermal simulations are not straightforward due to the convection phenomena induced by the stirrer and E-field spatial distribution [26]. This electromagnetic simulation permits to determine the spatial distribution of the E-field and to compare the numerical SAR averaged over the volume to the SAR obtained from the temperature measurements.

2.3. Experimental Dosimetry

Temperature measurements were carried out in order to investigate the temperature distribution inside the cuvette and the time dependence of the temperature at the optical beams level.

2.3.1. Principle

Experimentally, the SAR may also be assessed from temperature measurements. For sufficiently short time scales after the beginning of the exposure, the rate of temperature increase inside the sample is proportional to the rate at which energy is absorbed, until heat transfer can be neglected. Thus, the SAR can be expressed as:

$$SAR = C \left.\frac{\partial T}{\partial t}\right|_{t=t_{on}} \tag{4}$$

where C is the specific heat capacity of the sample ($4186\,\mathrm{J/(kg \cdot K)}$ for water at room temperature) and $\partial T/\partial t$ the time rate of temperature increase at t_{on}, i.e., the time at which the 2.45 GHz generator is turned on. The temperature measurements were achieved using a non-metallic temperature probe. This system is based on a fluoroptic fiber optic sensor which measures temperature. The sensor is immune to electromagnetic field and the probe is appropriate for temperature control of microwave processes and for temperature gradient mapping of fast temperature elevations. Typically, the time response is 0.25 s in stirred water. The fluoroptic sensor located at the end of the optic fiber has a diameter of 0.8 mm and a thickness of 0.2 mm. These characteristics allow measuring the temperature in a volume estimated around 1 to 2 mm^3. For the temperature measurements, four samples per second were recorded.

2.3.2. Measurements at Room Temperature

Real-time temperature measurements were recorded at 7 different positions (5 vertical positions with a step of 2.5 mm) inside the sample (Fig. 3). For each experiment, the microwave generator was turned on once thermal equilibrium was reached. The exposure time was set to 2 minutes and the input power was 3 W. The SAR values assessed from the temperature measurements were normalized to the incident power. This parameter is known as SAR efficiency (W/kg/W).

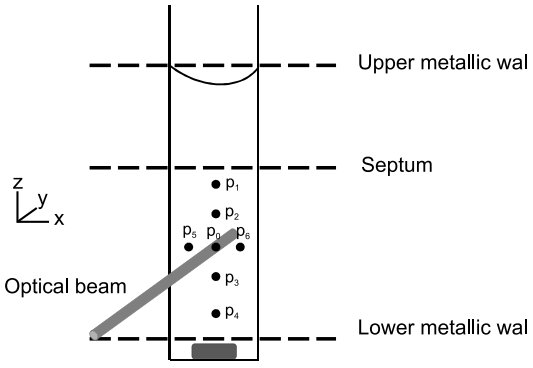

Figure 3. Schematic of the cuvette filled with water. The line defines the position of the excitation and emission optical beams. The dots define the positions at which the Luxtron probe was placed for temperature measurements (with a step of 2.5 mm).

In order to characterize the delivery system for a temperature rise above 25°C (which covers a temperature interval large enough around the expected phase transition temperature, allowing a good estimation of the latter parameter), measurements with a 10-fold higher input power (30 W) were also performed. To obtain a stabilized temperature in the cuvette and in the biological sample, the system was allowed to equilibrate for at least 30 minutes prior to EMF exposure. The exposure time was set to 12 minutes and the stirrer was turned on.

2.3.3. Measurements in Air-Conditioned Unit

As the gel-to-liquid crystalline phase transition temperature of lipid bilayers is 25°C–30°C depending on the constituents of the bilayer, experiments on the phase behavior of lipid bilayers were conducted from about 15°C to 45°C. To achieve initial temperatures lower than the room temperature, the TEM cell setup was installed inside an air-conditioned unit.

To verify that the SAR varies linearly with the input power, exposures were repeated with incident power ranging from 4 to 30 W. The exposure time was set to 2 minutes and the stirrer was rotating.

2.4. Fluorescence Measurements Protocol

Laurdan labeled SUVs were prepared according to [27]. Briefly, the phospholipid 1, 2-dimyristoyl-sn-glycero-3-phosphocholine (DMPC) was dissolved in chloroform, dried under nitrogen atmosphere to prevent oxidation, and resuspended in water at a final concentration of 2 mM. Laurdan stock solution in methanol was added at a final concentration of 2 μM and the sample was sonicated for 20 min. A volume of 2.8 ml of this suspension was introduced in the measuring cuvette. The Luxtron temperature probe was inserted in the central axis of the cuvette, 2.5 mm above the optical beams, and the system was left to equilibrate at 15°C inside the air-conditioned unit.

For the measurement of Laurdan emission spectra, the following conditions were used: $\lambda_{\text{excitation}} = 350\,\text{nm}$, $\lambda_{\text{emission-blue}} = 440\,\text{nm}$ and $\lambda_{\text{emission-green}} = 488\,\text{nm}$. The intensities at both emission wavelengths, I_{blue} and I_{green} respectively, were recorded at a 4 Hz sample rate, simultaneously with the temperature recording. The microwave power was applied after 2 min of temperature recording and the data acquisition continued until the temperature reached values of up to 45 °C.

The generalized polarization was then calculated according to [6, 7], using:

$$GP = \frac{I_{\text{blue}} - I_{\text{green}}}{I_{\text{blue}} + I_{\text{green}}} \tag{5}$$

Next, the SUVs suspension was heated by conventional heating to temperatures similar to those achieved with microwave heating. For that purpose, the cuvette containing the SUVs was placed inside the spectrofluorometer holder and heated through a Peltier unit. The Luxtron probe was used to monitor the temperature of the sample and the Laurdan emission spectra were recorded directly by the fluorometer.

3. RESULTS

3.1. Numerical Analysis

Figure 4 shows the E-field and the SAR distribution at 2.45 GHz in the cuvette filled with water placed within the TEM cell exposed to 1 W input power. The E-field is represented along X, Y, Z planes. The X, Y planes are considered in the middle of the structure while Z corresponds to the optical beam plane at half distance between the bottom grounded metallic wall and the septum of the TEM cell. As observed, the E-field is homogenous and restricted inside the TEM cell and only slightly modified by the presence of the cuvette filled with solution.

Without the cuvette, the field inside the TEM cell is proportional to the distance between the septum and the metallic wall. Due to the 50 Ω impedance of the structure, the E-field amplitude can be analytically assessed at around 600 V/m, for one watt incident power and considering the 12 mm gap. This value is consistent with those obtained by numerical simulation (Fig. 4(a)). With the cuvette filled with the solution, the E-field amplitude and spatial distribution change significantly. This is due to the

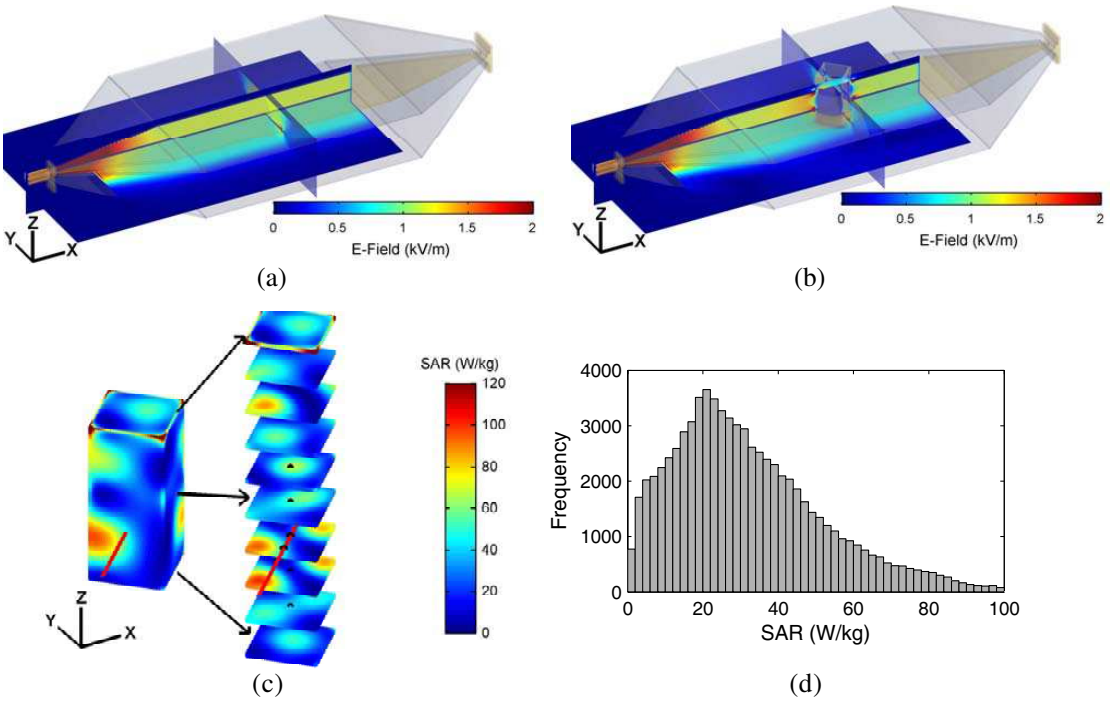

Figure 4. Numerical dosimetry at 2.45 GHz in the cuvette filled with water solution placed in the TEM cell. *E*-field distribution in the TEM cell (a) without and (b) with the cuvette, the distribution partially plotted for increased visibility of the TEM cell; (c) 3D SAR distribution external view of the solution in the cuvette and horizontal cuts of the SAR over the solution height captured every 2.5 mm, the temperature measurements points are represented as black dots, the red line corresponds to the optical beam; (d) SAR value histogram computed in the whole solution.

high relative dielectric constant and to the height of the solution. In order to increase the efficiency of the setup, the cuvette inside the TEM cell is filled from top to bottom metallic wall with a 2.8 ml sample. The equivalent wavelength in the solution is around 1.50 cm, which is smaller than the height of the solution. In such configuration, some resonant phenomena can occur in the sample inducing low homogeneity. This is highlighted on the distribution of the SAR over the cuvette volume and several horizontal cuts of the SAR over the solution height captured every 2.5 mm in Fig. 4(c). The locations of the experimental temperature measurements are represented as black dots.

The SAR value averaged over the entire volume was 30.4 W/kg and the standard deviation was 19.1 W/kg. The histogram shown in in Fig. 4(c) illustrates the SAR value distribution in the whole sample. Compared to the coaxial-based system [14] whose maximum SAR value was above 500 W/kg for 1 W input power, this delivery system has the advantage to produce SAR distributions that are more homogenous.

3.2. Experimental Measurements

3.2.1. Impedance Matching

The impedance matching to 50 Ω at 2.45 GHz of the TEM cell containing the cuvette was verified by measuring the *S*-parameters with a spectrum analyzer (HP 8753E, Agilent). The return loss, i.e., the S_{11}-parameter, was measured to be −17 dB at 2.45 GHz and less than −10 dB from DC up to 3 GHz (data not shown). Thus, good impedance matching was obtained with this system.

3.2.2. Dosimetry at Room Temperature

The SAR values obtained experimentally with an input power of 3 W are summarized in Table 1. The temperature increase was less than 2°C after the 2 min exposure time. The continuous stirring of the solution allowed homogenizing the temperature and the SAR distribution, hence the better homogeneity than that obtained in the numerical study. The SAR distribution was found to be homogeneous along the central axis and the plane containing the optical beams. The average SAR efficiency was found to be 27.5 ± 1.6 W/kg/W, which is in good agreement with the mean SAR efficiency (30.4 W/kg/W) computed from the numerical results and averaged over the entire sample. Compared to the literature, the efficiency of this delivery system was excellent [28].

Table 1. SAR values for 3 W input power for 2 min at room temperature and at different positions.

Position (relative to the optical beam)	SAR (W/kg)
P_0 (optical beam)	78.3 ± 4.6
P_1 (5 mm over optical beam)	88.6 ± 5.2
P_2 (2.5 mm over optical beam)	83.3 ± 4.4
P_3 (2.5 mm below optical beam)	76.9 ± 4.2
P_4 (5 mm below optical beam)	86.2 ± 4.6
P_5 (left of optical beam)	85.9 ± 6.4
P_6 (right of optical beam)	77.6 ± 4.8
Average ± std deviation (W/kg)	82.4 ± 4.8

Average ± standard deviation of the SAR efficiency is 27.5 ± 1.6 W/kg/W.

The temperature measurements recorded when the TEM cell was exposed to 30 W are shown in Fig. 5. Within the 12 minutes of exposure, a temperature increase of 28°C was achieved. As evidenced by the figure, the microwave-induced temperature increase exhibited an exponential increase, while the subsequent cooling followed an exponential decrease. This exponential variation is typical for systems that are subjected to heat transfer. The temperature increase is linear at the very beginning of the exposure, when the system can be considered adiabatic.

3.2.3. Dosimetry in Air-conditioned Unit

The temperature measurements obtained in the sample exposed within the air-conditioned unit are shown in Fig. 6. The SAR efficiency is similar for the four exposure conditions (4, 6, 10 and 30 W input powers), the average SAR efficiency of the system being 26.1 ± 2.1 W/kg/W. As expected, the SAR efficiency of the system in the air-conditioned unit was similar to that of the system left at room temperature.

3.2.4. Fluorescence Measurements

In Fig. 7, an example of fluorescence intensities measured on Laurdan labeled SUVs at 440 nm (I_{blue}) and 488 nm (I_{green}) is represented as a function of temperature between 15°C and 45°C. It can be seen that, as temperature rises, I_{blue} diminishes while I_{green} increases. This is due to the modification of the two spectral populations corresponding to different states of the fluorophore. The spectroscopic state emitting in blue corresponds to a non-hydrated state of Laurdan molecule, while the state emitting in green corresponds to a hydrated one. The ratio between these two populations expresses the stability of the lipid bilayer [6, 7].

In Fig. 8, the generalized polarization of the microwave exposed sample, calculated by Eq. (3), is represented versus temperature (grey line). For comparison, the black trace represents the GP versus temperature curve that was obtained when the sample was heated by conventional heating.

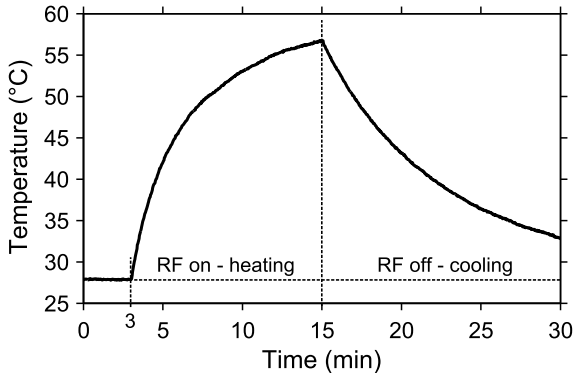

Figure 5. Experimental temperature measurements starting at room temperature. The generator is turned on at $t_{on} = 3$ minutes and turned off at $t_{off} = 15$ minutes. The input power is set to 30 W and the stirrer is turned on. This temperature measurement is made where with respect to the P_0 position

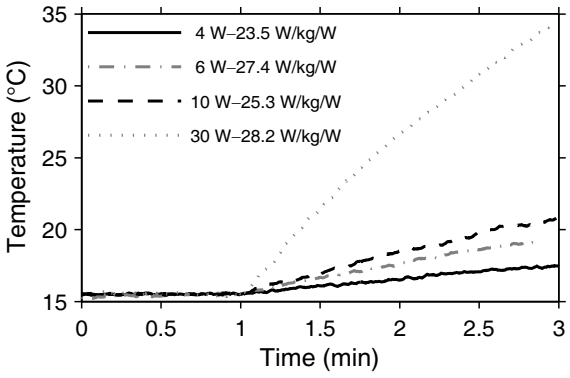

Figure 6. Initial temperature rise measured at the position of the optical beams for 4, 6, 10 and 30 W input power (the system is placed in the air conditioned unit and the stirrer is turned on).

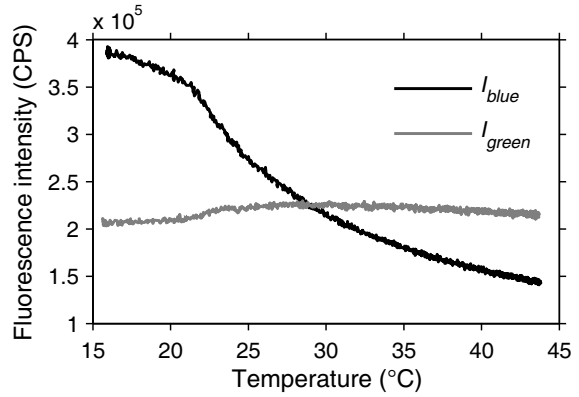

Figure 7. Fluorescence emission intensities of Laurdan measured as function of temperature using SUVs suspension exposed to 9 W input power.

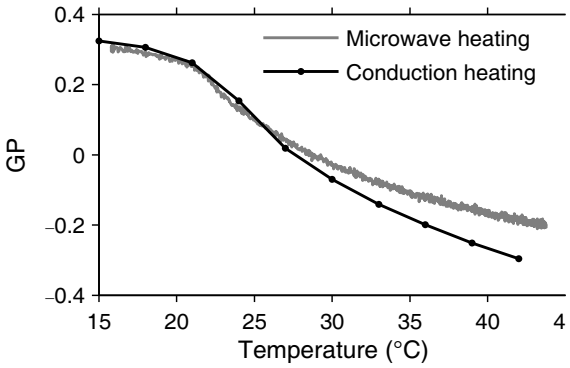

Figure 8. GP vs. temperature curves obtained in the TEM exposure system (Microwave heating) and in a standard heating experiment (Conduction heating). The SUVs suspension is exposed to 9 W input power or heating within the cuvette holder of the fluorometer.

The shape of the GP variations versus temperature is similar to that obtained in previous experiments [25].

The differences observed in the GP versus temperature curve at high temperatures (above 30°C), between the microwave and conventional heating conditions, may be due to direct interaction between the E-field and the lipid bilayers. This aspect will be the object of a further study.

4. CONCLUSION

The system described in this paper allowed simultaneous fluorescence measurements and well-controlled exposure of liquid biological samples to 2.45 GHz-electromagnetic fields. TEM cell was adapted with an optical guiding system that coupled the microwave exposure device to the monochromators and detectors of a spectrofluorometer.

For an accurate characterization of the system, rigorous numerical and experimental dosimetry was

conducted. The spatial distribution of the SAR in the cuvette filled with water was determined using an FDTD-based numerical tool. The experimental dosimetry of the system was carried out through temperature measurements under several exposure conditions (different positions of measurements in the cuvette, various input microwave powers, system at room temperature or in an air-conditioned unit). The results showed a good homogeneity of SAR values distribution in the area where fluorescence measurements were performed. With this system, a very good SAR efficiency of 26.1 ± 2.1 W/kg/W was obtained at 2.45 GHz.

In the previous system, the coaxial cable setup used as antenna was in close proximity to the biological sample, creating a hot spot with very high localized SAR values (values higher than 1800 W/kg for 1 W input power) [27]. In that case, the mean SAR value in the solution was around 500 W/kg for 1 W input power. In the current system, the electromagnetic field source is not in direct contact with the biological sample. The SAR efficiency of the coaxial cable system is larger than that of the TEM-cell based system. However, the development of hot spots in the new system is significantly reduced by using a crosshead magnetic stirrer that limited localized elevations in temperature.

Validation of the microwave exposure system was accomplished with biological experiments on SUVs involving fluorescence measurements at two different emission wavelengths. The generalized polarization of the SUVs membrane was obtained for different temperatures. The shape of the generalized polarization vs. temperature curve obtained using our system had a similar aspect as curves obtained directly in standard spectrofluorometers.

In this study, the proposed system was used for fluorescence measurements of generalized polarization on SUVs exposed to 2.45 GHz signals. Our exposure system has been developed to accommodate a spectrofluorometer allowing external measurements using an optical guiding system placed in direct contact with a cuvette. However, providing an accurate dosimetry, the setup can be successfully used in studies involving other types of fluorescence measurements (e.g., transmembrane potential, fluorescence resonance energy transfer, intracellular free Ca^{2+}, etc.) on different biological samples (small and giant unilamellar vesicles, cellular suspensions) while they are exposed to different microwave input powers (corresponding to different SAR levels) or to other signals such as those used in the wireless applications (GSM, UMTS, BAN, LTE).

ACKNOWLEDGMENT

Research conducted in the scope of the French-Romanian bilateral "Programme Hubert Curien Brancusi" and with the support of PNII grant IDEI 76/2010 (ID 7).

REFERENCES

1. Jones, D. A., T. P. Lelyveld, S. D. Mavrofidis, S. W. Kingman, and N. J. Miles, "Microwave heating applications in environmental engineering — A review," *Resources Conservation and Recycling*, Vol. 34, 75–90, Jan. 2002.
2. Kappe, C. O., "Controlled microwave heating in modern organic synthesis," *Angewandte Chemie-International Edition*, Vol. 43, 6250–6284, 2004.
3. Kappe, C. O. and D. Dallinger, "Controlled microwave heating in modern organic synthesis: Highlights from the 2004–2008 literature," *Molecular Diversity*, Vol. 13, 71–193, May 2009.
4. Mahrour, N., R. Pologea-Moraru, M. G. Moisescu, S. Orlowski, P. Leveque, and L. M. Mir, "In vitro increase of the fluid-phase endocytosis induced by pulsed radiofrequency electromagnetic fields: importance of the electric field component," *Biochimica Et Biophysica Acta-biomembranes*, Vol. 1668, 126–137, Feb. 2005.
5. Edidin, M., "Timeline — Lipids on the frontier: A century of cell-membrane bilayers," *Nature Reviews Molecular Cell Biology*, Vol. 4, 414–418, May 2003.
6. Parasassi, T., G. De Stasio, A. Dubaldo, and E. Gratton, "Phase fluctuation in phospholipid-membranes revealed by laurdan fluorescence," *Biophysical Journal*, Vol. 57, 1179–1186, Jun. 1990.
7. Parasassi, T., G. De Stasio, G. Ravagnan, R. M. Rusch, and E. Gratton, "Quantitation of lipid

phases in phospholipid-vesicles by the generalized polarization of laurdan fluorescence," *Biophysical Journal*, Vol. 60, 179–189, Jul. 1991.

8. Paffi, A., F. Apollonio, G. A. Lovisolo, C. Marino, R. Pinto, M. Repacholi, et al., "Considerations for developing an RF exposure system: A review for in vitro biological experiments," *IEEE Transactions on Microwave Theory and Techniques*, Vol. 58, 2702–2714, Oct. 2010.
9. Liberti, M., F. Apollonio, A. Paffi, M. Pellegrino, and G. D'Inzeo, "A coplanar-waveguide system for cells exposure during electrophysiological recordings," *IEEE Transactions on Microwave Theory and Techniques*, Vol. 52, 2521–2528, 2004.
10. Paffi, A., M. Pellegrino, R. Beccherelli, F. Apollonio, M. Liberti, D. Platano, et al., "A real-time exposure system for electrophysiological recording in brain slices," *IEEE Transactions on Microwave Theory and Techniques*, Vol. 55, 2463–2471, 2007.
11. Koester, P., J. Sakowski, W. Baumann, H.-W. Glock, and J. Gimsa, "A new exposure system for the in vitro detection of GHz field effects on neuronal networks," *Bioelectrochemistry*, Vol. 70, 104–114, 2007.
12. Lambrecht, M. R., I. Chatterjee, D. McPherson, J. Quinn, T. Hagan, and G. L. Craviso, "Design, characterization, and optimization of a waveguide-based RF/MW exposure system for studying nonthermal effects on skeletal muscle contraction," *IEEE Transactions on Plasma Science*, Vol. 34, 1470–1479, 2006.
13. Ramundo-Orlando, A., M. Liberti, G. Mossa, and G. D'Inzeo, "Effects of 2.45 GHz microwave fields on liposomes entrapping glycoenzyme ascorbate oxidase: Evidence for oligosaccharide side chain involvement," *Bioelectromagnetics*, Vol. 25, 338–345, 2004.
14. Kenaan, M., M. G. Moisescu, T. Savopol, D. Martin, D. Arnaud-Cormos, and P. Leveque, "Dosimetry of an in vitro exposure system for fluorescence measurements during 2.45 GHz microwave exposure," *International Journal of Microwave and Wireless Technologies*, Vol. 3, 81–86, Feb. 2011.
15. Kohler, S., R. P. O'Connor, V. Thi Dan Thao, P. Leveque, and D. Arnaud-Cormos, "Experimental microdosimetry techniques for biological cells exposed to nanosecond pulsed electric fields using microfluorimetry," *IEEE Transactions on Microwave Theory and Techniques*, Vol. 61, 2015–2022, 2013.
16. Ticaud, N., S. Kohler, P. Jarrige, L. Duvillaret, G. Gaborit, R. P. O'Connor, et al., "Specific absorption rate assessment using simultaneous electric field and temperature measurements," *IEEE Antennas and Wireless Propagation Letters*, Vol. 11, 252–255, 2012.
17. Merla, C., N. Ticaud, D. Arnaud-Cormos, B. Veyret, and P. Leveque, "Real-time RF exposure setup based on a multiple electrode array (MEA) for electrophysiological recording of neuronal networks," *IEEE Transactions on Microwave Theory and Techniques*, Vol. 59, 755–762, Mar. 2011.
18. O'Connor, R. P., S. D. Madison, P. Leveque, H. L. Roderick, and M. D. Bootman, "Exposure to GSM RF fields does not affect calcium homeostasis in human endothelial cells, rat pheocromocytoma cells or rat hippocampal neurons," *Plos. One*, Vol. 5, 16, Jul. 2010.
19. Moisescu, M. G., P. Leveque, J.-R. Bertrand, E. Kovacs, and L. M. Mir, "Microscopic observation of living cells during their exposure to modulated electromagnetic fields," *19th Biannual International Symposium on Bioelectrochemistry and Bioenergetics*, 9–15, Toulouse, France, 2007.
20. Taflove, A. and S. C. Hagness, *Computational Electrodynamics: The Finite-difference Time-domain Method*, 3rd Edition, Artech House, Boston, 2005.
21. Yee, K., "Numerical solution of initial boundary value problems involving Maxwell's equations in isotropic media," *IEEE Transactions on Antennas and Propagation*, Vol. 14, 302–307, 1966.
22. Leveque, P., A. Reineix, and B. Jecko, "Modeling of dielectric losses in microstrip patch antennas — Application of FDTD method," *Electronics Letters*, Vol. 28, 539–541, Mar. 1992.
23. Melon, C., P. Leveque, T. Monediere, A. Reineix, and F. Jecko, "Frequency-dependent finite-difference time-domain [(FD)(2)TD] formulation applied to ferrite material," *Microwave and Optical Technology Letters*, Vol. 7, 577–579, Aug. 1994.
24. Berenger, J. P., "A perfectly matched layer for the absorption of electromagnetic-waves," *Journal of Computational Physics*, Vol. 114, 185–200, Oct. 1994.

25. McKinlay, A. F., J. H. Bernhardt, A. Ahlbom, U. Bergqvist, J. P. Cesarini, M. Grandolfo, et al., "Guidance on determining compliance of exposure to pulsed and complex non-sinusoidal waveforms below 100 kHz with ICNIRP guidelines," *Health Physics*, Vol. 84, 383–387, 2003.
26. Cueille, M., A. Collin, C. Pivain, and P. Leveque, "Development of a numerical model connecting electromagnetism, thermal and hydrodynamics to analyse in vitro exposure system," *Annales Des Telecommunications — Annals of Telecommunications*, Vol. 63, 17–28, Feb. 2008.
27. Kovacs, E., T. Savopol, M. M. Iordache, L. Saplacan, I. Sobaru, C. Istrate, et al., "Interaction of gentamicin polycation with model and cell membranes," *Bioelectrochemistry*, Vol. 87, 230–235, Oct. 2012.
28. Schuderer, J., D. Spat, T. Samaras, W. Oesch, and N. Kuster, "In vitro exposure systems for RF exposures at 900 MHz," *IEEE Transactions on Microwave Theory and Techniques*, Vol. 52, 2067–2075, 2004.